

Table S2 – List of primers

Primers		Sequence
VP40-31	forward	TAATACGACTCACTATA GATGAAGATTAAGAAAAAGAGGGATTTTCTC
	reverse	GAGAAAATCCCTCTTTTCTTAATCTTCATC TATAGTGAGTCGTATTA

Primers were used to synthesize VP40 sequence-specific RNAs by *in vitro* transcription using the HiScribe T7 High Yield RNA Synthesis Kit (NEB).

Figure S1 – Alignment of mononegavirus MTase+CTD domains.

Alignment of the MTase+CTD domain of *Sudan ebolavirus* (SUDV; accession code YP_138527.1) with those of other members of the *Filoviridae* family [*Zaire ebolavirus* (EBOV; AAG40171.1), *Tai Forest ebolavirus* (TAFV; ALT19766.1), *Bundibugyo ebolavirus* (BDBV; YP_003815440.1), *Reston ebolavirus* (RESTV; APA16576.1), *Marburg marburgvirus* (MARV; P35262) and *Lloviu cuevavirus* (LLOV; YP_004928143.1)], as well as members of the *Paramyxoviridae* family [Sendai virus (SeV; P06447), Measles virus (MeV; BAB60955.1), Hendra virus (HeV; O89344) and Mumps virus (Muv; P30929)], the *Rhabdoviridae* family [Rabies virus (RabV; ABZ81226.1), vesicular stomatitis virus (VSV; ABP01784.1)] and the *Pneumoviridae* family [human respiratory syncytial virus (hRSV; AAX23996.1), human metapneumovirus (hMPV; AGJ74101.1)]. The alignment was generated using T-Coffee⁶⁸ and MAFFT⁶⁹ software, taking into account available structural information (PDB codes 4UCI for hMPV, 5A22 for VSV). It was visualised using ESPript 3x⁷⁰. WebLogo⁷¹ was used to illustrate degrees of conservation of amino-acids (shown underneath the alignment). The numbering on top of the alignment indicates amino-acid positions in the *Sudan ebolavirus* sequence, the red dots highlight the K-D-K-E motif, the bent arrow indicates the approximate start of the CTD. Spirals and arrows underneath the alignment indicate positions of helices and β -strands in the hMPV structure.

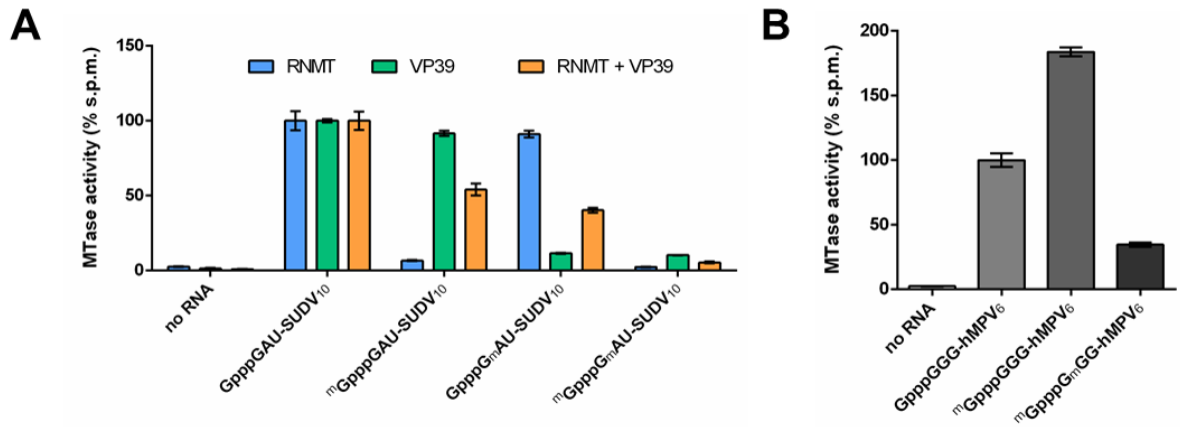


Figure S2 - Cap MTases reveal specific activity on the cap structure.

(A) RNMT (human N7 MTase) and VP39 (vaccinia virus 2'O MTase) activity on a set of capped, synthetic SUDV sequence-specific RNAs (13mers), with methylated residues at different positions (Gppp: cap, ¹⁴Cppp: N7-methylated cap, G_m: 2'O-methylated residue). Groups have been normalized to the highest activity measured for HO-(A)₂₇ (n=3). Data represent normalized mean ± standard deviation. (B) hMPV MTase activity measurement on a set of synthetic hMPV sequence-specific RNAs (13mers) with methylated residues at different positions (Gppp: cap, ¹⁴Cppp: N7-methylated cap, G_m: 2'O-methylated residue) mimicking 5' cap structures. Groups have been normalized versus unmethylated control (n=6). Data represent normalized mean ± standard deviation.

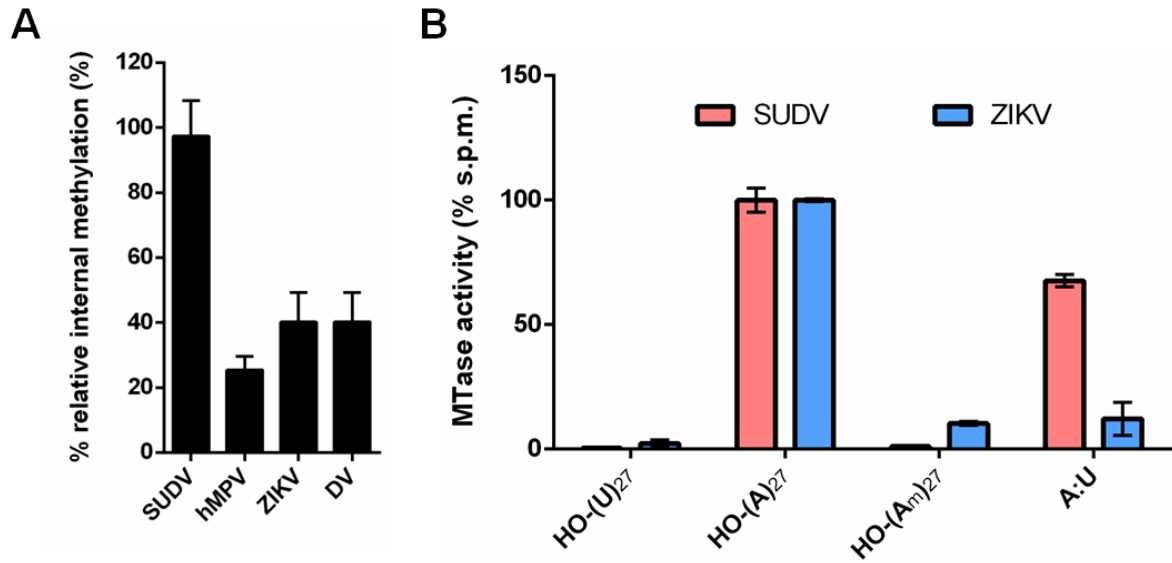


Figure S3 – Internal 2'O methyltransferase activity is a specific feature of SUDV MTase.

(A) Ratios of methyltransferase activities on cap-1 RNAs (^mGpppX_m-RNA) over those on capped but unmethylated RNAs (GpppX-RNA) for MTase domains of *Sudan ebolavirus* (SUDV), *Human metapneumovirus* (hMPV), *Zika flavivirus* (ZIKV) and *Dengue flavivirus* (DV). RNA sequences were virus-specific. Values represent mean ratio ± standard deviation. (B) Comparison of MTase activity profiles of SUDV and ZIKV MTase domains on different synthetic homopolymeric RNAs and a equimolar mix of HO-(A)₂₇ and HO-(U)₂₇ (A:U). Groups have been normalized versus highest signal measured for HO-(A)₂₇ (n=3). Data represent normalized mean ± standard deviation.

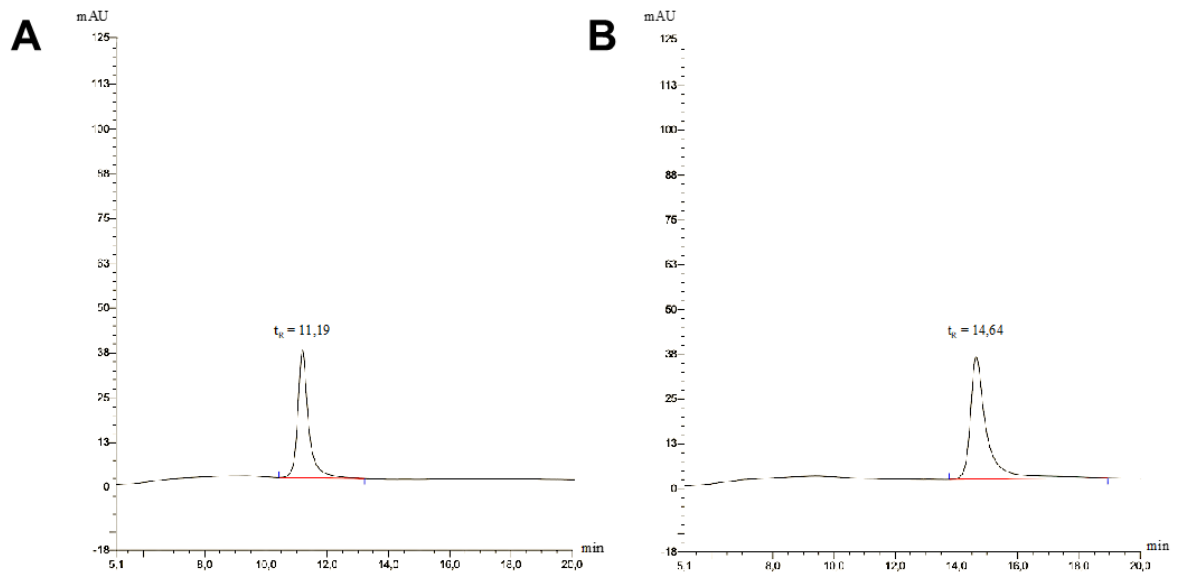


Figure S4 - HPLC controls for adenosine and 2'O-methylated adenosine identification.

(A) HPLC profile of HO-(A)₂₇ treated with snake venom phosphodiesterase and alkaline phosphatase. The adenosine (2'OH-A) control eluted after 11.2 min under the conditions of the experiment. (B) HPLC profile of HO-(A)₂₇ digested with snake venom phosphodiesterase and alkaline phosphatase. The 2'O-methylated adenosine (2'OCH₃-A) control eluted after 14.6 min.

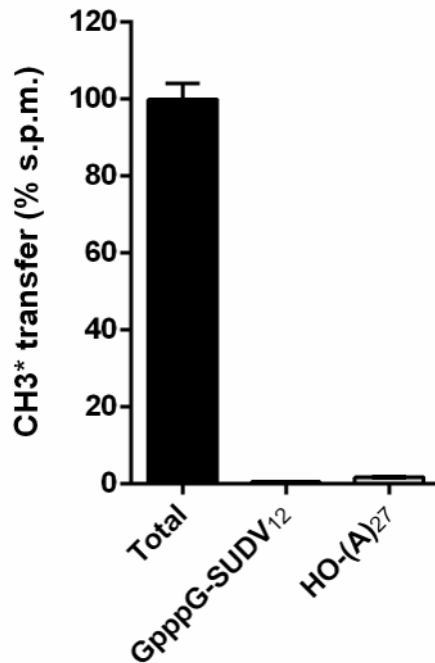


Figure S5– Evaluation of methyl transfer by MTase assay on different RNA substrates.

Total radioactivity (Total) corresponds to the radioactivity of 2 μM of radioactive SAM (SAM*) in the reaction mix volume used in the assays. The methyl transfer was measured in the presence of 2 μM of SAM* onto two RNAs (at 10 μM concentrations): a synthetic, SUDV sequence-specific, 13-mer RNA with a cap (GpppG), and a 27-mer polyadenosine (HO-(A)₂₇). Groups have been normalized versus « Total » control (n=3). Data represent normalized mean \pm standard deviation.

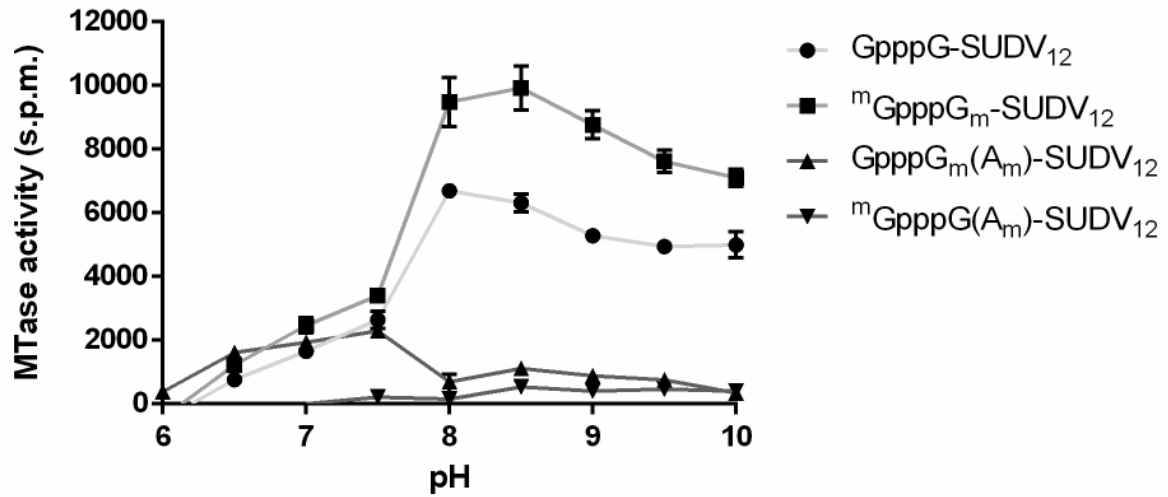


Figure S6 - N7 and 2'O MTase reactions have a different optimal pH.

Sudan ebolavirus (SUDV) L protein methyltransferase domain (MTase) flanked by the C-terminal domain (CTD) methyltransferase activity evaluation at different pHs (from 6.0 to 10.0) on a set of synthetic SUDV sequence-specific RNAs (13-mers) as indicated in the figure.

Supplementary References

68. Notredame, C., Higgins, D. G. & Heringa, J. T-Coffee: A novel method for fast and accurate multiple sequence alignment. *J. Mol. Biol.* **302**, 205–217 (2000).
69. Katoh, K., Misawa, K., Kuma, K. & Miyata, T. MAFFT: a novel method for rapid multiple sequence alignment based on fast Fourier transform. *Nucleic Acids Res.* **30**, 3059–3066 (2002).
70. Robert, X. & Gouet, P. Deciphering key features in protein structures with the new ENDscript server. *Nucleic Acids Res.* **42**, W320-324 (2014).
71. Crooks, G. E., Hon, G., Chandonia, J.-M. & Brenner, S. E. WebLogo: a sequence logo generator. *Genome Res.* **14**, 1188–1190 (2004).